FIFTH INTERNATIONAL CONGRESS ON SOUND AND VIBRATION
DECEMBER 15-18, 1997
ADELAIDE, SOUTH AUSTRALIA

Specialist Keynote Paper

ACOUSTIC VARIABILITY AND SONAR

Adrian D. Jones

Maritime Operations Division
Aeronautical and Maritime Research Laboratory
Defence Science and Technology Organisation
PO Box 1500, Salisbury SA 5108
AUSTRALIA
Email: adrian.jones@dsto.defence.gov.au

ABSTRACT

The performance of sonar systems, particularly in shallow ocean areas typical of a continental shelf, is complicated and limited by the variability of the acoustic signals which are received. Here, signals vary over time, with spatial location and with frequency, often in ways that are poorly understood. The present state of knowledge of this acoustic variability is reviewed, and some recent developments which have de-mystified some aspects of the phenomena are described. As is shown, average descriptions of the variation of signals with frequency, position and time may be determined, based on the properties of the acoustic signal field. It is shown how these descriptions suggest that the performance of sonar systems may be optimised. It is also shown how these descriptions lead to the specification of parameters for system performance and effectiveness modelling.

1. INTRODUCTION

Sonar variability is an all-encompassing term describing the occurrence of fluctuations of both the signals and noise received in the underwater environment. Most components of this variability have their cause attributable to this underwater environment, however, some variability may be imposed by a direct variation in the signal level of the sound source. This paper considers, primarily, the environmentally induced components of variability.

Variability affects anti-submarine warfare (ASW) and anti-surface vessel warfare (ASuW) sonar systems by limiting their ability to detect, classify and track target signals. It limits the ability of sonar arrays to discriminate between signals and noise. The variability of signals and noise gives rise to the uncertainty in the sonar detection range - hence the sonar community deals with probabilities of detection, and a source to receiver range has a level of detection probability associated with it. Rather than being a curse, however, variability presents sonar system designers and operators with the potential for system performance

enhancement through anticipation of its effects and a matching of the setup and deployment of each sonar system to the measured, or expected, environmental peculiarities - a true exploitation of the sonar environment.

Many of the characteristics of variability, and some of the mechanisms for its exploitation for ASW and ASuW are reviewed below. Particular reference is made to the effects of variability in ducted transmission environments, including the shallow ocean regions of a continental shelf and the isothermal mixed layer which may exist at the surface of an ocean of any depth.

1.1 Causes of variability

Signals and noise received in the ocean fluctuate with changes in location (**spatial variability**), with changes in frequency (**spectral variability**) or with changes in time (**temporal variability**), due to underlying mechanisms. However, due to the constant motion of the sound source and receiver, the target (for active sonar), the body of the ocean, and the ocean surface, these forms of variability are often assumed to be, and studied as, temporal in nature (this is how Urick [1] considers the problem). Thus, variability tends to be classified in relation to the timescale of its observance, although it must be studied according to the underlying mechanisms. These mechanisms are explained below. Variability is then often classified as:

- very short term - changes within an integration time ~ seconds to a few minutes
- short term - changes over a time ≥ integration time
- medium term - changes over a period ~ hours
- long term - changes over a period longer than a sonar encounter, up to annual climate cycle

1.2 Ducted Transmission - Interference

Ducted transmission environments are important in regard to the operation of sonar systems. In deep oceans, sonar encounters often take place within mixed layer ducts. Continental shelf areas, between about 50 to 200 m deep, constitute acoustic ducts under all circumstances. For a sound source and a receiver both within an acoustic duct, numerous transmission paths exist. It is the acoustic interference between these paths which causes much of the observed spatial and spectral variability. Further, temporal changes of these transmission paths, and of the associated acoustic interference, cause much of the observed temporal variability.

As shown in Figure 1, surface ducted transmission is caused by upward refraction. Here, the mixing of the ocean in the surface layer creates isothermal conditions and the rise in sound speed with pressure (and depth) causes the refraction (see, for example, Urick [1]).

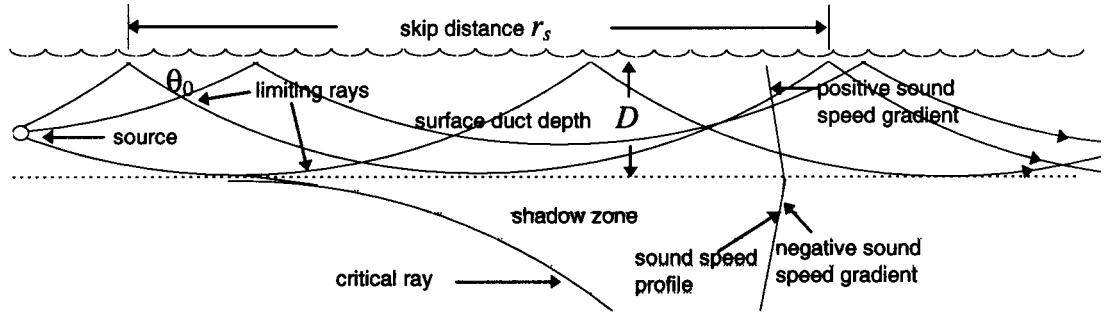

Figure 1: Sound transmission in a mixed layer surface duct

Shallow oceans usually involve some measure of refraction, but for simplicity, Figure 2 depicts an isovelocity ocean, with straight line ray paths. In practice, any one of a wide range of refractive conditions may exist, but, of course, up to some close range limit, refractive effects are small, and straight line transmission is a good approximation.

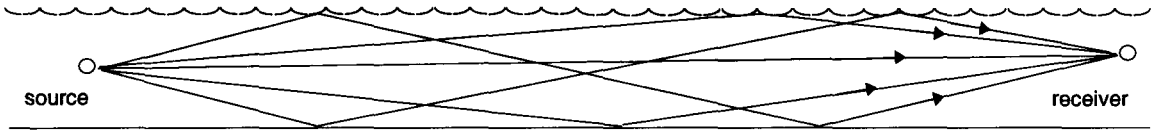

Figure 2: Sound transmission in an isovelocity shallow ocean

1.3 Lloyd Mirror - Interference

A limiting case of underwater acoustic interference exists between a direct path arrival and the surface reflection - the Lloyd mirror (e.g. section 5.7 of Urick [1]). Figure 3 shows the transmission paths. This is relevant in deep oceans at ranges for which refractive effects are not strong, and at similar ranges in shallow oceans with non-reflective seafloors. The Lloyd mirror variability of transmission with range, depth and frequency may be predicted deterministically, but the signal fluctuations are often considered within an overall variability.

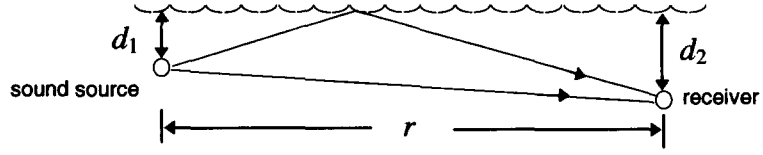

Figure 3: Sound transmission resulting in Lloyd mirror interference

2. SPATIAL VARIABILITY - TRANSMISSION LOSS

For ocean environmental conditions which cause ducted transmission, a large component of variability is spatial in nature. In these circumstances, at each single frequency, the sound source creates an interference field which moves as it does. Thus the sonar receiver passes through the detail of the interference field as the range to the source changes, and the received level at a given frequency fluctuates. This is experienced as short term and medium term temporal variability of the transmission loss (*TL*). Figure 4 shows an example of *TL* versus range in km, in which characteristic spatial fluctuations are evident.

Figure 4 shows *TL* computed for 500 Hz, with source depth 12.2 m, receiver depth 30 m, in a 75 m deep ocean with downward refraction to a reflective seafloor. Clearly, a spatially-correlated random variability exists about the incoherent mean. This spatial variability may be defined by a non-dimensional distance Δx_r, being the range in wavelengths for the autocorrelation of linear pressure amplitude to decay a specified amount. By inspection of Figure 4, this distance is of the order of 0.2 km at the closer ranges, giving $\Delta x_r \sim 70\lambda$. As shown below, this autocorrelation distance, Δx_r, tends to be frequency-independent, as it is related to the angular distribution of signal energy arriving at each point in the acoustic field. Clearly, a timescale imposed by this spatial variability is entirely dependent on the relative range rate between the source and the receiver, Δx_r and the acoustic wavelength. For 5 knots range rate at 500 Hz, the timescale corresponding with $\Delta x_r \sim 70\lambda$ is ~ 1.2 minutes.

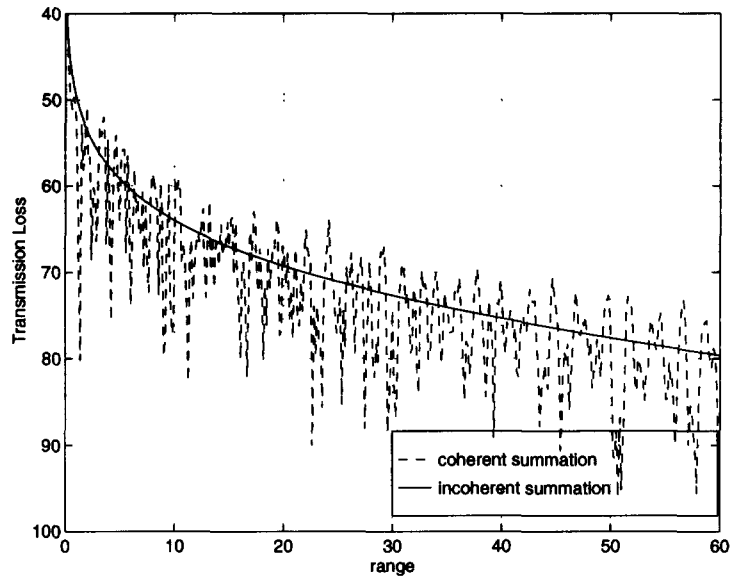

Figure 4: Coherent, incoherent *TL* at single frequency in shallow ocean

2.1 Spatial Variability in Highly Muli-Path Duct

In a multi-path duct, the interference field is formed by the coherent summation of the acoustic pressure values contributed by each of the separate transmission paths. At a given location in the field, the coherently summed acoustic pressure is constant in amplitude and phase, relative to the emission at the source. However, for slightly different receiver depth or range, the combining arrivals give a slightly different coherent summation.

At very low frequencies, transmission is not highly multi-modal. Ray theory is not valid (see, for example, Etter [2]) and few generalisations will be possible. At higher frequencies, there will be many modes of transmission, ray theory may be applied and statistically based solutions are possible. Here, multi-path arrivals will combine like a large number of vectors of somewhat randomly different amplitude and phase. The central limit theorem will apply to the summation, and, as shown by, for example, Urick [3], the distribution of the signal amplitude envelope versus range (or depth) is either Rayleigh or Rician, depending on whether there is one dominant path.

2.2 Numerical Simulation of Interference Field

2.2.1 Transmission simulations

Using an isovelocity ray-based transmission model for a shallow ocean scenario, Jones et al [4] showed that both the radial and vertical spatial scales of amplitude variability were linked to changes in the environment which impacted on the angular distribution of signal power arriving at the receiver: increasing range; decreasing ocean depth; increased ocean bottom acoustic absorption. Each of these factors caused the spatial scale of the variability, in both the radial and the vertical direction, to increase.

2.2.2 Field simulation model

Jones et al [4] used a model of an arbitrary tonal signal field to study the link between the angular distribution of arrivals and the spatial variability. Here, various distributions of arrival power versus elevation angle were selected, and the spatial variability was derived

numerically. A large number of ray arrivals (1000) was assumed to intersect at a point. Each arrival was constrained to the vertical plane containing the receiver, and was assumed to correspond with a plane wave of infinite extent and unchanging amplitude. The field was simulated by using the plane wave equation to calculate the phase advance.

2.2.3 Field simulations

The angular distributions of incident signal power were based on that obtained from an isovelocity ray-based transmission model for a particular case: frequency 1 kHz, ocean depth 100 m, source depth 12 m, receiver depth 18 m, range 10 km, ocean bottom reflection coefficient 0.6 (bottom loss 4.4 dB). This distribution of incident power, nominally over ± 6°, is shown in Figure 5, with the resultant simulation of the radial and vertical signal amplitudes.

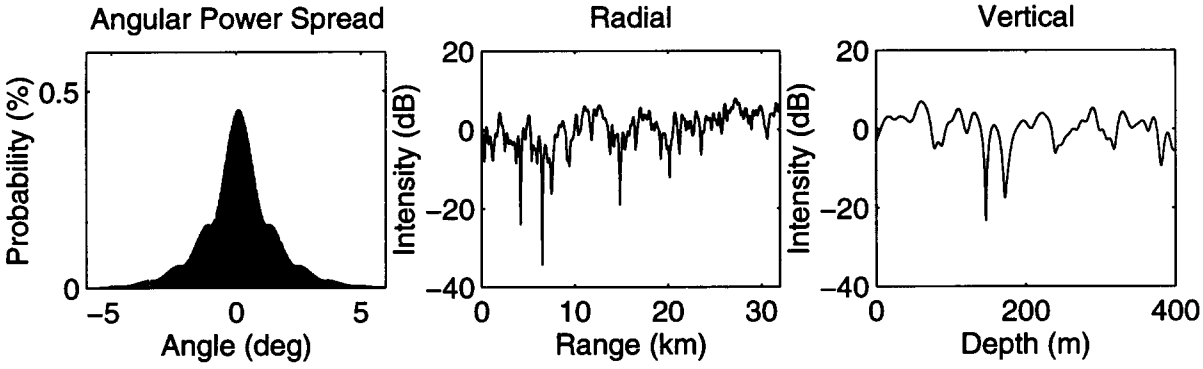

Figure 5. Simulation of sound pressure amplitude variability, ± 6° angular spread, 1 kHz

A further batch of simulations was carried out for different angular distributions of incident power. Here, each angular distribution was obtained from that for the ± 6° case, Figure 5, with a simple expansion or contraction on the angular axis to, in turn, ± 3°, ± 12°, ± 24°.

2.2.4 Spatial autocorrelation function

For each simulation, the normalised spatial autocorrelation function of the received sound pressure amplitude, or modulus, $\rho_{|p|}(\Delta x)$, was determined from the data [4], and the distances Δx_r, Δx_v, associated with the 0.8 and 0.6 values of the autocorrelation coefficient, for radial and vertical displacement, respectively, were determined. The autocorrelation was carried out on the modulus of the sound pressure expressed relative to the average modulus, that is, on $|p(x)| - \langle |p(x)| \rangle$. The normalised autocorrelation of this zero-mean sound pressure modulus is

$$\rho_{|p|}(\Delta x) = \frac{\langle |p(x)||p(x+\Delta x)| \rangle - \langle |p(x)| \rangle^2}{\langle |p(x)|^2 \rangle - \langle |p(x)| \rangle^2} \tag{1}$$

2.3 Correlation Length

2.3.1 Effect of Frequency

Based on simulations described in section 2.2.3, the spatial autocorrelation function was determined for the six octave centre frequencies from 125 Hz to 4 kHz, for the ±6° angular spread of incident acoustic power [4]. As shown in Figure 6, the autocorrelations are very similar, especially to the 0.8 level of correlation. From these data, each of the radial and vertical de-correlation distances is independent of frequency.

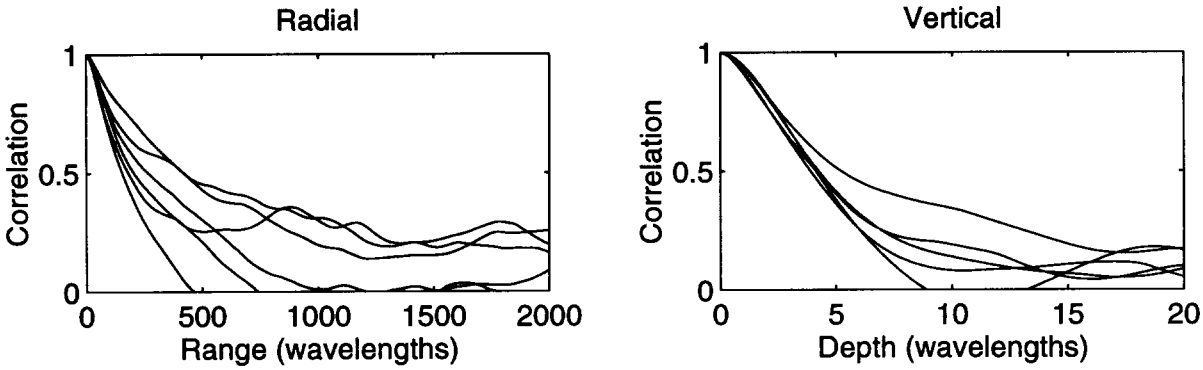

Figure 6. Spatial autocorrelation, ± 6° angular spread, octave frequencies 125 Hz to 4 kHz

2.3.2 Effect of Angular Spread of Incident Acoustic Power

For the four angular distributions of section 2.2.3, the spatial autocorrelation function was determined, for a single frequency. The de-correlation distances, in wavelengths, are shown in Table 1, for radial displacement, and in Table 2 for vertical displacement [4].

Table 1. Amplitude de-correlation distance, Δx_r, wavelengths, radial displacement [4]

	Angular Spread of Incident Acoustic Power			
Correlation Coefficient	±3°	±6°	±12°	±24°
0.8	375	75	25	6.7
0.6	-	145	42	11

Table 2. Amplitude de-correlation distance, Δx_v, wavelengths, vertical displacement [4]

	Angular Spread of Incident Acoustic Power			
Correlation Coefficient	±3°	±6°	±12°	±24°
0.8	4.6	2.1	0.80	0.40
0.6	7.5	3.3	2.1	0.87

These results show a clear relationship between the angular distribution of incident energy and the de-correlation lengths Δx_r and Δx_v. Further, the data in Table 1 indicate an inverse square law dependence of de-correlation length on angular spread, whereas data in Table 2 indicate an inverse linear relationship. These relationships may be explained by considering the amplitude variability as the result of beating between closely spaced spatial frequencies along either the radial or the vertical directions [4].

The ocean environmental conditions which will narrow the angular spread of incident acoustic power in shallow oceans, or surface ducted transmission, and thus lengthen the spatial scales of variability Δx_r and Δx_v, are as follows:

- absorbing (non-reflecting) seafloor, or duct boundary
- at range ≤ skip distance[1] - increased source-to-receiver range
- surface ducted transmission - reduced duct depth

[1] see Figure 1 for depiction of skip distance

- shallow ocean transmission - reduced seafloor depth
- at range > skip distance - reduced magnitude of sound speed gradient

2.3.3 Maximum array lengths

It is expected [4] that amplitude de-correlation lengths, derived as described above, may be used to specify the maximum practical length of an array - as linked to the local acoustic environment. Further, such determinations might be based on *in situ* data.

2.3.4 Modal approach

With a modal rather than ray description of transmission, amplitude spatial variability has been considered as the result of interference between normal modes (e.g. section 6.7.2 of Brekhovskikh and Lysanov [5]). The modal description is essential if transmission is not highly multi-modal. However, where ray theory is valid, the angular distribution of the arrival signal energy is the preferred means of description as generalised solutions become available.

2.3.5 Lloyd mirror

For Lloyd mirror interference (Figure 3), the spatial variability is readily determined. The radial spacing, Δx_r, between adjacent nulls, for a sound speed c, may be shown to be

$$\Delta x_r = \frac{c\, r^2}{2 f\, d_1 d_2} \tag{2}$$

2.4 Amplitude of Spatial Variability

For highly multi-modal ducted transmission, the received signal values, in terms of rms sound pressure versus range, tend to be Rayleigh distributed about the incoherent mean (section 2.1). Thus, the amplitude of *TL* variability, in terms of a standard deviation σ of logarithmically displayed values, is about 5.6 dB (e.g. Pierce [6] section 6-7). This value is consistent with the span of fluctuations ($\pm 2\sigma$ span expected) shown in Figure 4 for the coherent summation.

If the ducted transmission is bounded by a non-reflective lower boundary (seafloor or surface duct boundary), the progressive loss of signal with range may change the standard deviation of the fluctuations. A significant signal loss at the duct boundary may, for ranges $\leq$ the skip distance, cause the interference to approach that for Lloyd mirror, for which the standard deviation σ is about 16 dB [7]. However, at longer ranges with a non-reflecting boundary, the refraction ensures that the less direct paths are greatly attenuated. This type of transmission tends to have one dominant arrival, and a reduced amplitude of variability. Generally, the more acoustically dead[2] the underwater environment, the longer is Δx_r and Δx_v and the lower is the σ of the fluctuations. In these circumstances, or at close ranges to the source, the single dominant transmission path causes the fluctuation probability distribution to be Rician, rather than Rayleigh. The σ for the fluctuations is then related to the randomicity of the received signal. Randomicity is defined (Urick [1], page 190) as the ratio of mean squared sound pressure from the random paths $\overline{p_r^2}$ to the total mean squared sound pressure from all paths $\overline{p_t^2}$. Values of σ in these circumstances are shown in Table 3 [9].

[2] e.g. see Beranek [8] chapter 9, for the concept of an acoustically dead room

Table 3: Variability standard deviation σ for Rician fluctuations

randomicity $\overline{p_r^2}/\overline{p_t^2}$	σ dB	randomicity $\overline{p_r^2}/\overline{p_t^2}$	σ dB
1.0	5.6	0.1	2.0
0.5	4.9	0.0588	1.5
0.2	3.0	0.0385	1.2

2.4.1 Target size

For some circumstances, submarine targets have length and height greater than the de-correlation lengths Δx_r and Δx_v, respectively. For example, a submarine of 50 m length and 9 m height has a length of 100 wavelengths at 3 kHz and a height of 3 wavelengths at 500 Hz. Clearly, from the values of Δx_r and Δx_v in Table 1 and Table 2, at mid-kHz frequencies, for a ±6° angular spread of arrivals, the different sections of the target will be insonified with different amplitudes of signal. If a determination may be made of the number, N, of independent arrivals, the overall standard deviation σ of transmission spatial variability is that for a single arrival divided by $\sqrt{N}$.

3. SPECTRAL VARIABILITY - TRANSMISSION LOSS

For each ocean environment in which an acoustic interference field exists, the received signals exhibit fluctuations of amplitude and phase according to:

- variations of source or receiver range and depth (fixed source frequency)
- variations of signal frequency (fixed source and receiver location)

The former phenomenon is spatial variability, as considered above. The latter is spectral variability. Spectral variability thus describes the environmentally induced difference between the received amplitudes and phases of signals transmitted simultaneously at differing frequencies from a given source to a given receiver.

The degree of spectral variability may be expressed as the frequency scale Δf over which significant changes in acoustic transmission occur. As shown below, in a highly multi-path environment typical of a surface duct, and shallow oceans with reflective seafloors, the phenomenon, and its description, is statistical in nature, and is linked to the time for the significant multiple paths of sound to combine.

Virtually none of the literature describes spectral variability in ocean sound transmission. In fact, neither Urick [1], nor Etter [2] give expressions for spectral variability for the Lloyd mirror case. Here, the spacing between either adjacent nulls or adjacent peaks, Δf_L, for a sound speed c, may be shown to be [7]

$$\Delta f_L = \frac{c\, r}{2\, d_1\, d_2} \tag{3}$$

3.1 Transmission Loss as a Transfer Function

By considering the ocean as linear filter system, and by suitable scaling, the phase coherent *TL*, displayed as amplitude versus frequency, may be equated with the amplitude of the

transfer function between two points, $|T(f)|$. This transfer function may be determined by measurement of the received signal $p_2(t)$ from a known transient source $p_1(t)$:

$$\text{transfer function } T(f) = \frac{\text{Fourier transform of output } p_2(t)}{\text{Fourier transform of input } p_1(t)} \tag{4}$$

Alternatively, $T(f)$ may be found as the Fourier transform of the impulse response $P(t)$. In practice, $T(f)$ might be determined using a known transient, such as a SUS[3] charge. Usually, however, the exact determination of *TL* versus frequency is not available and practical considerations must be limited to the average statistical characteristics of the *TL*.

3.2 Spectral Variability in a Highly Multi-Path Duct

As mentioned in section 2.1, the combining signal arrivals, in highly multi-modal transmission situations, may be considered as summing vectors of randomly different amplitude and phase. Small frequency changes will cause the vectors to rotate relative to each other. With a sufficient change in frequency, the vector sum will have a significantly different amplitude. Intuitively, one may see that the time separation between arrivals, and the relative amplitudes of the arrivals will determine the frequency change required for a significant change in the vector sum. With few high amplitude arrivals, and with small time differences, the amplitude of the sum is relatively insensitive to frequency change. Conversely, large time differences and large numbers of arrivals give a sum that is extremely frequency-sensitive. Corresponding ocean environments are, respectively, acoustically dead and acoustically live.

The link between spectral variability and the time for the combination of significant multi-paths was established by Schroeder [10] in relation to room acoustics. Jones and Hoefs [9] applied the same approach to sound transmission in a water-filled tank, and Jones et al [7] applied it to transmission in a shallow ocean. Such a link is to be expected, as the statistical nature of the transfer function and of *TL* versus frequency, might be presumed to be related to the statistical nature of the impulse response - this being a characteristic decay rate.

3.3 Reverberant decay time

For highly multi-modal or multi-path transmission, the sound field may be characterised by the time τ for significant combination of the arrivals, that is, the time for the interference field to establish. Thus, τ is a parameter which encompasses the effect of both multi-path length differences and transmission losses along the multiple paths. Significantly, τ is effectively the same as for the decay of the interference field following cessation of insonification [11].

The time τ may be defined as that for the acoustical energy density at the receiver to decrease by a factor e^4 (same as time for sound intensity at receiver to decay by e) on cessation of insonification. An alternative term is the "reverberation time", T_{60}, for 60 dB drop (i.e. a decrease by a factor of 10^6)[5]. For an exponential decay

$$T_{60} = \left(6 \ln(10)\right) \tau \approx 13.82\, \tau. \tag{5}$$

---

[3] Signals, Underwater Sound - an explosive noise source for underwater use

[4] e is the base of natural logarithms, 2.71828

[5] The terms τ and T_{60} are identical with those used in room acoustics [6].

Random multi-path environments are then characterised by either τ or T_{60}. For transmission situations with one dominant arrival, plus a large number of random multi-paths, there will be an initial very rapid decay, as the direct path drops out, followed by a more gradual decay. Here, the more gradual decay is associated with the times τ or T_{60}. Thus the concept of the decay rate applies to transmission situations with either Rayleigh or Rician statistics.

3.4 Frequency-Autocorrelation Function of Pressure Amplitude

From Schroeder [10], the normalised frequency-autocorrelation function of the amplitude, or modulus, of the frequency response, $\rho_{|p|}(\Delta f)$, may be expressed in terms of τ, as follows:

$$\rho_{|p|}(\Delta f) \approx \frac{1}{1+(2\,\pi\,\tau\,\Delta f)^2} \quad \text{where } \Delta f \text{ is the frequency interval involved} \tag{6}$$

Here, the autocorrelation is carried out on the modulus of the sound pressure expressed relative to the average modulus of the frequency response, that is, on $|p(f)| - \langle |p(f)| \rangle$. The normalised autocorrelation of this zero-mean sound pressure modulus is

$$\rho_{|p|}(\Delta f) = \frac{\langle |p(f)|\,|p(f+\Delta f)| \rangle - \langle |p(f)| \rangle^2}{\langle |p(f)|^2 \rangle - \langle |p(f)| \rangle^2} \tag{7}$$

From equation (6), the $1/e$ point in the autocorrelation is at a frequency displacement Δf_e, as

$$\Delta f_e \approx \frac{\sqrt{e-1}}{2\,\pi\,\tau} \approx \frac{2.88}{T_{60}} \text{ Hz} \tag{8}$$

3.5 Frequency displacement for independence

The frequency displacement Δf_e is indicative of that required for a significant change in received signal amplitude level. However, a more useful quantity, a frequency displacement Δf_i for statistical independence of received signal amplitude levels, may be obtained, based on Schroeder's considerations [12] of the standard deviation σ of the averaged sound pressure amplitude, in dB SPL (sound pressure level), of signals received across a frequency band.

For any highly multi-modal transmission situation, the variability of the pressure amplitude response to a change in frequency, is according to the Rayleigh distribution. As discussed in section 2.4, the received signal amplitude values, expressed on a logarithmic scale (as SPL), have a standard deviation, $\sigma \approx 5.6$ dB. From Schroeder [12], the standard deviation, σ, of the frequency-averaged logarithmic response is reduced as a function of $B \times \tau$ or $B \times T_{60}$, where B is the averaging bandwidth:

$$\sigma \approx \frac{5.6}{\sqrt{1+3.3\,\tau\,B}} \approx \frac{5.6}{\sqrt{1+0.238\,T_{60}\,B}} \text{ dB} \tag{9}$$

Now, if these reduced fluctuations were the result of averaging over N independent measurements, the resulting standard deviation would be $\sigma = 5.6/\sqrt{N}$ dB. Thus, from equation (9), frequency averaging corresponds with making $1+3.3\,\tau\,B$ (or $1+0.238\,T_{60}\,B$) independent measurements. Frequency spacing for independence then corresponds with the

minimum value of B which gives two independent samples. Thus, the frequency separation Δf_i for independence of spectrally sampled received signal amplitude levels in dB is given by:

$$\Delta f_i \approx \frac{1}{0.238\, T_{60}} \approx \frac{4.2}{T_{60}} \text{ Hz} \tag{10}$$

In practice, T_{60} will be frequency dependent, but equations (8) and (10) are valid so long as the values of Δf_e and Δf_i are small compared with the frequency range over which T_{60} changes.

For a Rician sound channel, it is expected that equations (8) and (10) are approximately valid. This follows, as the decay of the sound field, following the drop-out of the dominant path, will be as in a Rayleigh sound channel. Thus, the *TL* versus frequency response will have a scale of variability according to Δf_e and Δf_i, but with a reduced fluctuation σ.

3.6 Spectral Variability Observed in Shallow Ocean Transmission

The appropriateness of the above concept of spectral variability has been validated with sonar data obtained by the Maritime Operations Division [7]. Here, both swept tone (LFM) pulses and pure tone (CW) pulses were transmitted within seconds of each other in a multi-path shallow water environment. Each received LFM pulse included substantial fluctuations in amplitude within the pulse duration, whilst received CW pulses were much less distorted. Below, it is shown that local measurements of the time for the multi-path interference field to establish were linked via equation (8) to the observed distortions of the LFM pulses. This confirms that transmission variability induced by a variation with frequency may be estimated from a knowledge of the sonar environment.

3.6.1 Distortion of LFM pulses in shallow ocean environment

Figure 7 shows the envelope of the rms sound pressure amplitude, in dB SPL, for a LFM pulse received at 2 nm range in a shallow ocean of 85 m depth [7]. The emitted pulse comprised a one-second duration sweep from 6.3 kHz to 6.7 kHz. The sweep rate was linear (400 Hz/s), and the emitted pulse amplitude was uniform. Source depth was 90 ft and receiver depth 60 ft.

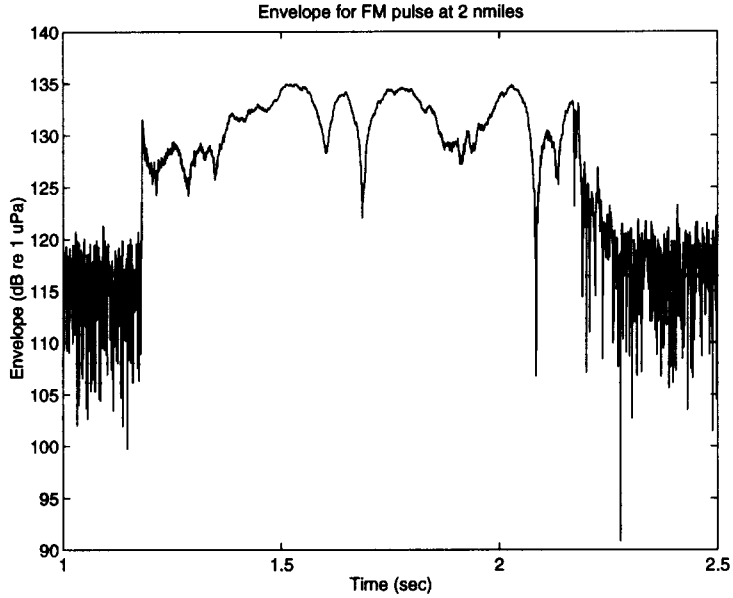

Figure 7. Envelope of rms sound pressure amplitude throughout received LFM pulse (2 nm)

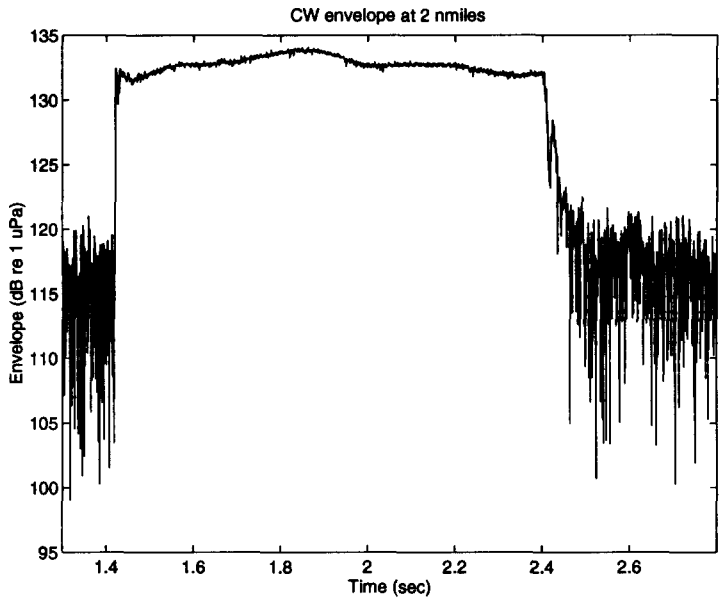

Figure 8. Envelope of rms sound pressure amplitude throughout received CW pulse (2 nm)

The effect of the transmission environment on a CW signal is shown in Figure 8, for a one-second duration 6.5 kHz emitted pulse, for the same source-receiver combination. The received pulse exhibits a slight envelope distortion. This is consistent with a slight spreading of the frequency of the transmitted signal, due to small Doppler shifts induced by the specular reflection from the moving sea surface, and due to the motion within the body of the ocean.

Intuitively, it does seem that the much greater amplitude fluctuations in Figure 7 are caused by multi-path induced spectral variability. Further, these fluctuations do have the appearance of frequency-correlated Rayleigh distributed values. In fact, the standard deviation of the pressure amplitude values shown within the received pulse of Figure 7 is 5.55 dB, compared to an expected 5.6 dB for a Rayleigh distribution and highly multi-path transmission.

3.6.2 Sound field decay

Toward the end of each emitted pulse, insonification is terminated rapidly [7]. Thus, the irregular tail observed on the end of each of the received pulses is due to the decay of the interference field generated by the pulse. The time for the sound field to decay, in terms of T_{60}, was then estimated from an enlargement of the trailing edge of a received pulse. Based on the trailing edge of received CW pulse (Figure 8), T_{60} was estimated as 0.20 seconds.

3.6.3 Frequency-autocorrelation function of measured pressure amplitude

The normalised autocorrelation function of the amplitude of the frequency response was determined by applying equation (7) to the within-pulse data in Figure 7 [7]. Here, each particular time within the received pulse duration was assumed to correspond with a single frequency[6]. The frequency displacement Δf_e was determined as the point at which this derived autocorrelation fell to $1/e$ [7]. This value of Δf_e, labelled "measured", is shown in Table 4, together with the measured reverberation time T_{60} and the frequency displacement Δf_e determined from equation (8) using that value of T_{60}.

[6] This was appropriate, as the frequency span Δf swept within the effective time for the sound field to be established (τ approximates this time) was small in relation to Δf_e.

Table 4: Measured, calculated frequency displacements for spectral variability

	2 nm range
T_{60}, based on received CW pulse	0.20 s
Δf_e, measured, based on received LFM pulse	18 Hz
Δf_e, calculated ($2.88/T_{60}$)	14.4 Hz
Δf_i (Δf_e, measured, $\times 4.2/2.88$)	26 Hz

From Table 4, the frequency interval Δf_e at which the received signal amplitude frequency-autocorrelation decreases to $1/e$ is very close to the value derived from a measurement of the decay time T_{60}. Clearly, the statistics of spectral shaping of swept tone pulses may be related to the time for the multi-path interference field to establish. The value Δf_i shown in Table 4, indicates the minimum spectral separation required for statistical independence of *TL*.

3.7 Implications of Spectral Variability

A characteristic time, τ or T_{60}, for a highly multi-path interference field to establish to a significant degree is a single parameter by which the statistics of random variability of received amplitude with frequency may be completely specified. This has implications for the transmission of both broadband and narrowband signals in multi-path environments. Broadband signals will be "coloured" according to Rayleigh or Rician amplitude variations, with a frequency scale of spectral features of the order of Δf_e given by equation (8). Narrowband signals at differing frequencies will have correlated or uncorrelated signal amplitude fluctuations, depending on their frequency of separation and Δf_i given by equation (10). Even in the presence of spatial or temporal variability, received tonal signals will have correlated amplitudes if their frequency of separation is significantly less than Δf_i.

Values of τ or T_{60} may be estimated for different scenarios, using appropriate transmission models, or measurements from similar situations. These times will be reduced, and the frequency scale of spectral variability will be increased if there is reduced reflection at ocean boundaries, or if there is a decrease in the length differences of the acoustic multi-paths. For isovelocity transmission, the frequency scale of spectral variability Δf_i will increase with:

- increased surface or bottom loss
- increased range to receiver
- reduced ocean depth

4. TEMPORAL VARIABILITY - TRANSMISSION LOSS

In a real ocean, movement of the surface and the volume will change the multi-paths which generate the interference field. Such movement will alter the field and give rise to fluctuations which are temporal in nature - temporal variability. The variability timescale is dependent on the proportion of the received signal energy which travels via reflections from the fast-moving surface, and the proportion which travels via the more slowly moving body of the ocean. The surface motion exists with a period of ~ 10 seconds, whereas internal waves within the ocean have periods between the buoyancy or Brunt-Väisälä frequency of, at

minimum, about 6 minutes, and the inertial frequency of about 24 hrs (see Etter [2], page 42). For littoral waters, the tidal cycle causes ocean depth changes, and affects transmission paths.

4.1 Coherent Transmission

If the characteristic time, t_c, for the ocean transmission paths to change is much greater than the time, τ, for the interference field to form, the multi-path contributions will always produce a coherent sum. If the reverse is true, that is, if $(t_c/\tau) \ll 1.0$, then the multi-path arrivals do not combine with a fixed phase relationship - the transmission is incoherent.

The time t_c may be assumed to be that corresponding to a $\pm\pi/2$ phase change along a transmission path. Clearly, t_c will tend to be less for long ranges or high frequencies, where transmission occurs over many wavelengths, and for which a small perturbation of the ocean medium greatly alters the interference field. The time τ will tend towards frequency independence, so, in general, the ratio (t_c/τ) will decrease with increasing range, and increasing frequency, with transmission becoming progressively incoherent.

4.2 Amplitude of Temporal Variability

For highly coherent transmission, (for which $(t_c/\tau) \gg 1$), the received signal amplitude values will be temporally correlated random samples from the same distribution which is obtained in the case of either spatial movement or frequency variation. This may be understood by regarding the received multi-path signal components as summing vectors. It is the vectors that determine the distribution - the variability is either spatial, spectral or temporal.

In many cases, the transmission paths do not undergo a temporal phase change of as much as $\pi/2$. For temporal phase changes $\ll \pi/2$, the signal amplitude vector sum will be drawn from a subset of the distribution obtained with a full random combination of arrivals. In general, this subset of values will result in the standard deviation σ of the received signal amplitude values in dB being less than that obtained with full random variability.

For partially coherent transmission, the combined received signal will resemble a sinusoid contaminated by noise. The variability standard deviation σ will be reduced as the presence of the noise-like incoherent signal will reduce the occurrence of drop-outs.

In the event of a change in the sound speed versus depth profile over time, or a change of some feature of the ocean environment which changes the incoherent mean *TL* curve, a medium or long term variability will be imposed over whatever shorter term variability exists. The total variability of *TL* in these circumstances will then be greater than for the standard deviation σ expected for unchanged environment.

5. AMBIENT NOISE VARIABILITY

Within different frequency bands, ocean ambient noise is usually dominated by one of weather effects (wind/wave, rain), biological sources (fish, crustaceans, cetaceans) or shipping (e.g. Urick [1], ch. 7). In the event of very large numbers of individual sources, the central limit theorem implies that the time series is Gaussian. In fact, ocean ambient noise is usually

considered as quasi-stationary Gaussian (Urick [1], section 7.7). Thus, for the time period of a sonar integration, the noise is statistically stationary, but over the medium term and long term, the mean level changes due to weather, biological and shipping effects. Thus, the noise level (*NL*) term in the sonar equation may be regarded as having very short term and short term variability as sampled from a stationary Gaussian random input. Medium term and long term variability of *NL* originate in changes to the mean level, and the associated standard deviation is best determined from historical data for the local environment.

Ambient noise values, over the period in which the noise is stationary, may be regarded as uncorrelated samples from a χ^2 distribution with $2\,w\,t$ degrees of freedom, where w is the analysis bandwidth in Hz, and t is the sonar integration time, seconds [13]. A single sample, for which $w\,t = 1$, is then drawn from a distribution with the same standard deviation of variability σ as the Rayleigh distribution, 5.6 dB[7]. The values of σ, in dB, for other values of $w\,t$ may be found, approximately, based on Table II of Blackman and Tukey [14], as:

$$\sigma \approx \frac{25}{4\sqrt{2\,w\,t - 1}} \text{ dB} \tag{11}$$

If shipping noise is dominant, the number of vessels causing the noise becomes relevant. With few vessels, the variability may be modelled as that due to transmission. Here, the number of spectral lines within the analysis bandwidth w, and the independence of the transmission paths for those tones, will determine the overall variability standard deviation. With k spectral lines within bandwidth w, for Rayleigh transmission variability at each frequency, and for statistically independent transmission at each tonal frequency, the resultant variability for large k follows as:

$$\sigma \approx \frac{25}{4\sqrt{k - 1}} \text{ dB}^{8} \tag{12}$$

The variability timescale for shipping noise may be determined from a knowledge of the transmission spatial variability (see section 2) at each tone, and the relative speed of each ship.

6. INPUTS TO MODELLING

The performance, and effectiveness, of a sonar system may be greatly influenced by the acoustic variability phenomena described above, and these variability effects must be properly accounted for in modelling studies. For example, the amplitude of variability of received signal to noise determines the span of ranges at which detections occur. The frequency scale of variability determines the independence of detection opportunities at different tonals. Further, processing of sonar signals for detection, classification and tracking will be limited by each of spatial, spectral and temporal variability. Significant issues are reviewed below.

6.1 Sonar Performance Modelling

Detection is assumed to occur at the range, or ranges, at which signal excess (SE) ≥ 0 [1]. SE is given by the sonar equations, as follows:

$$\text{passive } SE = SL - TL - NL + DI - DT \tag{13}$$

$$\text{active } SE = SL - 2\,TL + TS - NL + DI - DT \tag{14}$$

---

[7] The squares of Rayleigh distributed random samples are χ^2 distributed with 2 degrees of freedom.

[8] Note that equation (12) resembles the $\sigma = 5.6/\sqrt{N}$ relation postulated in section 3.5.

In the event that the acoustic source level (*SL*), *NL*[9], directivity index (*DI*), target strength (*TS*) and detection threshold (*DT*) are all fixed, and *TL* increases with range, the sonar equation will be satisfied (*SE* = 0.0) at just one range value - this is the detection range. But, of course, noise samples are continually varying, the target *SL* or *TS* may be varying, and the *TL* has fluctuations as described in sections 2, 3 and 4. Thus each range value has a spread of *SE* values associated with it. Clearly, the target is detectable at many ranges, with a greater or lesser probability of detection, *Pd*, at each range. The greater the *SE* variability, the greater the spread of ranges at which a detection is possible - variability determines detectable range.

Detection theory has resulted in techniques that provide a value of *Pd* for each value of *SE*, for a particular probability of false alarm, *Pfa*. Curves which link values of *Pd* and *Pfa* to different values of *SE* are known as **receiver operating characteristic** (ROC) curves, these being effectively the same as **transition curves** (see, for example, Urick [1] ch. 12). It is common to use log-normal transition curves [1], for convenience. These link each value of *SE* in dB to a value of *Pd* via what is, in fact, the cumulative distribution curve for a Gaussian of standard deviation σ equal to the overall assumed sonar variability standard deviation in dB. In this way, the overall variability of *SE*, for each of equations (13) and (14), is assumed to be log-normally distributed. The so-called "0.0 dB transition curve" (e.g. Urick [1], Fig. 12.10) contains that variability due to random fluctuations of stationary noise, only.

The standard deviation, σ_{SE}, of the overall variability of *SE* in dB, must be obtained for each particular modelling exercise, so that the appropriate transition curve may be selected. If all fluctuations are assumed independent, the overall variability is obtained by adding the variability from each term, as follows:

$$\text{passive } \sigma_{SE}^2 = \sigma_{SL}^2 + \sigma_{TL}^2 + \sigma_{NL}^2 + \sigma_{DI}^2 \tag{15}$$

$$\text{active } \sigma_{SE}^2 = \sigma_{SL}^2 + \sigma_{TL}^2 + \sigma_{TS}^2 + \sigma_{NL}^2 + \sigma_{DI}^2 \tag{16}$$

In the case of active sonar, with two way transmission, the overall variability in *TL* is dependent on whether the transmission paths are the same each way. If not, then the total σ_{TL} is found by assuming independence, as in equation (16). If the paths are similar, the two way variability depends on the covariance between the terms, as

$$\sigma_{TL}^2 = \sigma_{TL1}^2 + \sigma_{TL2}^2 + 2\,\mathrm{cov}\left(\sigma_{TL1}^2, \sigma_{TL2}^2\right) \tag{17}$$

If the transmission paths are the same

$$\sigma_{TL}^2 = 2\left(\sigma_{TL1}^2 + \sigma_{TL2}^2\right) \tag{18}$$

For example, if each of σ_{TL1} and σ_{TL2} are 5.6 dB, for independent forward and reflected paths, σ_{TL} is 7.9 dB. If the forward and reflected paths are the same, σ_{TL} is 11.2 dB.

It must be noted that the *TL* variability must not be counted twice. If the *TL* versus range data is smoothed (to the incoherent sum[10] [2]), σ_{TL} must include the total transmission variability. However, if the *TL* data is semi-smoothed, σ_{TL} must include the residual variability, only - part of the variability is retained in the *TL* versus range data which is used to determine *SE*.

---

[9] For active sonar equation, reverberation level (*RL*) may be included with noise level

[10] For use with log-normal transition curves, *TL* values obtained by incoherent summation of random multi-paths must be increased by 2.5 dB.

6.2 System Effectiveness Modelling

The effectiveness with which a particular maritime operation is carried out by a vessel or aircraft, or by of a force of vessels and/or aircraft, equipped with particular sonar systems, is often modelled with Monte Carlo simulations of the tactical scenario. In this way, various measures of effectiveness of a sonar system, or of its use, may be determined by repeatedly simulating the sonar encounter, with the appropriate events in each simulation randomly selected from amongst the respective possible distributions. With a very large number of simulations of the sonar encounter, as many as 1000 or so, statistically significant measures of effectiveness may be determined. An important part of this process is the proper selection of variability parameters for input to the model. Depending on the scenario, and the model being used, the variability probability distributions, the amplitudes of variability components, plus the spatial, spectral and temporal scales of variability will be required as inputs. Sections 2, 3, 4 and 5 outline the techniques by which each of these variability inputs may be selected.

An MOD study considered the importance of the correct choice of variability inputs. As an example, a simulation of an aircraft using a passive sonar system in a search for a submarine gave values of 0.17, 0.28 or 0.39 for the probability that the submarine would be detected within the search duration, depending on whether the variability timescales were modelled as long (days), medium (hours) or short (minutes), respectively. One practical implication of this result is that the variability timescale, which might be either medium term or short term, depending on the spatial scale of the interference field and the closing speed of the submarine to sonar sensors (see Figure 4, and section 2), must be modelled appropriately.

7. SONAR SYSTEM OPTIMISATION

The optimisation of the configuration, setup and operation of sonar systems to the local ocean environmental conditions is an area of much present research. Broadly, there are two approaches to this optimisation: adaptation to mean environmental conditions; exploitation of the statistics and/or detail of the underwater signal interference field and underwater noise field. Knowledge of acoustic variability, as outlined above, is essential to the latter techniques of system optimisation.

The fluctuation of received signals with spatial location, often perceived as temporal variability, gives particular potential for optimisation. For example, for a given sonar receiver, or receiver array, it is preferable to match the processing integration time to that time for which the signal will be received with a constant intensity. As indicated in section 2, with the aid of Figure 4, this time may be estimated from a knowledge, or determination of the spatial scale of variability within the underwater interference field. Conversely, the selection of the length of a horizontal array may be linked to a maximisation of the processing integration time according to the spatial interference field-induced temporal variability. Further, the maximum practical length for a vertical array may be chosen to correspond with the signal amplitude de-correlation length, Δx_v, described in section 2.3.2.

Possible technologies for optimisation of ASW and ASuW sonars to local ocean environmental conditions are many, but include:

- determination of maximum lengths over which coherent beamforming may be employed,
- determination of maximum duration for synthetic aperture array processing,

- knowledge of practical array gain,
- minimum spectral and spatial separations for use in matched field processing,
- optimisation of data integration time,
- inference of source disposition, ocean environment from signal field measurements,
- selection of time interval between sonar pulses,
- preferred bandwidth of a sonar signal.

Without elaboration here, operational implications of these technologies include:
- optimisation of spatial deployments of signal sources and sonar receivers,
- optimisation of signal processing for towed array sonars, fixed seabed array sonars,
- source range/depth determination from single sensor or sensor array,
- *in-situ* determination of ocean environmental properties (e.g. seafloor reflection loss).

8. CONCLUSION

Acoustic variability has significant effects on the performance of sonar systems. Variability causes, on the one hand, enhancement to the sonar detection range, e.g. through constructive addition of multi-path signals, and on the other hand gives an ultimate limitation to the performance of a sonar system. Until recently, some variability phenomena were not well understood. In the case of surface-ducted or shallow ocean transmission environments, recent insights into the cause and nature of acoustic variability, as outlined above, do give the promise that the performance of ASW and ASuW sonar systems might be understood, modelled accurately, and hence optimised, and that a knowledge of the local underwater environment might be exploited by new sonar system designs and methods of operation.

Section 2 of this paper reviewed how the spatial scale of variability of received signal amplitude levels has been linked to the angular distribution of the signal energy which is incident at a receiver. For small angular spreads of arrival energy, typical of shallow oceans and surface ducts in deep oceans, the statistics of spatial variability are predictable. Here, the spatial scale for radial displacement, Δx_r, is large, and is inversely proportional to the square of the angular spread of arrival energy. The corresponding spatial scale in the vertical direction, Δx_v, is shorter, and is inversely proportional to the angular spread of arrival energy.

Section 3 reviewed how the spectral statistics of variability of received signal amplitude have been determined for a highly multi-path acoustic environment. Here, the average frequency spacing for independent transmission of tonal signals is related to the time, τ, or T_{60}, for the interference field to establish to a significant degree. This parameter may be determined from a knowledge of the environment, and of the source and receiver depths and separation range.

The world of sonar systems is changing in both the approach to signal processing (the "dry end") and in the types of acoustic hardware (the "wet end") being designed. Rather than basing receiver design and signal processing on the assumed receipt of signals via a single plane wave transmission within an ocean of isotropic, stationary, Gaussian noise, it is now recognised that transmission is via a series of multiple paths of predictable amplitudes, time delays and angles of arrival, and that there are real possibilities of exploiting the expectation of this phenomena. Ultimately, this might be done using techniques of great sophistication, with intensive use of signal processing power, and a matching to the exact detail of the signal

field. In the first instance, however, there is much potential to anticipate and exploit the statistical nature of the sonar variability, as outlined above.

The configuration of acoustic projectors and receivers for sonar systems is also undergoing change. Acoustic frequencies used for each of passive and active sonar are becoming lower, and array sizes are becoming larger, in the eternal hunt for an increased, or maintained, detection range against ever quieter and more anechoic targets. For each of passive and active sonar systems, the multi-path nature of transmission in each of surface ducts and shallow oceans becomes more relevant and exploitable as the frequency is reduced, as the array size is increased and as the detection range increases. Hence, a knowledge of, and an ability to predict and exploit the signal acoustic interference field is becoming progressively more important. Again, the techniques outlined above, of describing the signal interference field, will become more and more relevant as both sonar "dry end" and "wet end" designs progress.

REFERENCES

1. Urick, Robert J. *Principles of Underwater Sound*, 3rd edition, McGraw-Hill, 1983
2. Etter, Paul C., *Underwater Acoustic Modeling: Principles, Techniques and Applications*, Elsevier Science Publishers Ltd. 1991
3. Urick, R. J. *A Statistical Model for the Fluctuation of Sound Transmission in the Sea* Technical Report 75 - 18, Naval Surface Weapons Center, White Oak, Silver Spring, Maryland, February 1975
4. Jones, A. D.; Harrison, S. and Zerk, D. *Acoustic Spatial Variability in Ducted Ocean Environments*, draft DSTO Research Report
5. Brekhovskikh, L. M. and Lysanov, Yu. P. *Fundamentals of Ocean Acoustics* 2nd edition, Springer-Verlag, 1991
6. Pierce, Allan D. *Acoustics - An Introduction to Its Physical Principles and Applications* Acoustical Society of America, 1989
7. Jones, A. D.; Lourey, S. J. and Larsson, A. I. *Spectral Variability in Sonar* draft DSTO Research Report
8. Beranek, L. L. *Noise and Vibration Control*, McGraw-Hill, 1971
9. Jones, A. D. and Hoefs, S. A. *Acoustical Properties of the MOD Salisbury Test Tank and Techniques for Measurements*, DSTO Research Report, DSTO-RR-0068, AR-009-476, January 1996
10. Schroeder, M.R. *Frequency-Correlation Functions of Frequency Responses in Rooms*, J. Acoust. Soc. Am., Vol. 34, No. 12, December 1962, pp 1819-1823
11. Schroeder, M.R. *Complementarity of Sound Buildup and Decay* J. Acoust. Soc. Am., Vol. 40, No. 3, 1966, pp 549-551
12. Schroeder, M.R. *Effect of Frequency and Space Averaging on the Transmission Responses of Multimode Media* J. Acoust. Soc. Am., Vol. 46, No. 2 (Part 1), 1969, pp 277-283
13. Urick, R. J. *Models for the amplitude fluctuations of narrow-band signals and noise in the sea* J. Acoust. Soc. Am., Vol. 62, No. 4, October 1977, pp 878-887
14. Blackman, R. B. and Tukey, J. W. *The Measurement of Power Spectra*, Dover, 1959